Effect of ZnO nanosizing on its solubility in aqueous media

Jindřich Leitner[1], *David Sedmidubský*[2], *Ondřej Jankovský*[2] ✉

[1]*Department of Solid State Engineering, University of Chemistry and Technology Prague, Technická 5, 166 28 Prague 6, Czech Republic*
[2]*Department of Inorganic Chemistry, University of Chemistry and Technology Prague, Technická 5, 166 28 Prague 6, Czech Republic*
✉ *E-mail: Ondrej.Jankovsky@vscht.cz*

Published in Micro & Nano Letters; Received on 11th May 2018; Revised on 29th June 2018; Accepted on 11th July 2018

Zinc pollution represents a great environmental risk, particularly with regards to the aquatic environment. In this theoretical contribution, the enhanced solubility of ZnO nanoparticles in pure water is predicted based on a simple thermodynamic model. The study used Zn^{2+}, $Zn(OH)^{+}$, $Zn(OH)_2$, $Zn(OH)_3^-$ and $Zn(OH)_4^{2-}$ as dominant species in aqueous solution and a Gibbs energy minimisation method to calculate equilibrium Zn content in this solution. ZnO was investigated in the form of nanoparticles of various shapes, whose very high surface-to-volume ratio implicates their lower thermodynamic stability compared with bulk material. The interfacial energy of the solid ZnO – dilute aqueous solution interface was assessed by applying the average ZnO surface energy and contact angle of a sessile drop of water on ZnO(0001)-O surface. At 298 K, the ratio of 2 nm spherical ZnO particles to the bulk material solubility was about 23.7. The calculated results were compared with experimental data and yielded a good agreement. These results are not only of great importance for nanomaterials research but they also have implications for environmental protection.

1. Introduction: Zinc(II) oxide is a widely used material in rubber manufacturing (more than 50% of all production), ceramics industry, medicine and cosmetics, coatings, pigments and so on [1]. Zinc also plays a key role in nature. In low concentrations, it is an essential trace element not only for humans and animals but also for plants and microorganisms [2, 3]. However, in high concentrations, zinc can be extremely dangerous because it is very toxic to aquatic organisms and may cause long-term adverse effects in the aquatic environment [4–6].

The enhanced solubility of nanoparticles is one of the numerous consequences of reducing the size of matter. This behaviour of small (nano-) particles was predicted more than a century ago. Following Gibbs treatment of interfaces and their consequent influence on the equilibrium between solid particles and a liquid solution, the Ostwald–Freundlich equation

$$\ln\frac{c_{A,r}}{c_{A,\infty}}=\frac{2\gamma_{sl}V_{m,A}}{RTr} \tag{1}$$

was derived [7, 8], where $c_{A,r}$ and $c_{A,\infty}$ represent the equilibrium solubility of a substance A in the form of spherical particles of radius r and bulk material ($r\to\infty$), respectively, and where γ_{sl} is the interfacial energy between a solid particle and solution. Equation (1) holds for an ideal solution of A in a solvent and assumes that the interface energy γ_{sl} is not radius dependent. The enhanced solubility caused by nanosizing is of great importance in many fields of chemistry, physics and materials science, including environmental chemistry, biochemistry and pharmaceutical technology.

Due to its wide variety of applications, zinc oxide (ZnO) belongs to a group of materials whose size-dependent solubility and dissolution rate in various aqueous media have been widely investigated [4, 9–21]. Regardless of solvent and temperature, solubility increases as particle size decreases. The aim of this work is to predict enhanced ZnO nanoparticle solubility in pure water. This prediction results from Gibbs description of interfaces and is based on calculating the composition of an aqueous solution in thermodynamic equilibrium with solid ZnO nanoparticles. The interface effect is included and the value of relevant interface energy estimated on the basis of contact angle measurement.

2. Thermodynamic description of ZnO dissolution

2.1. Dissolution of bulk ZnO: The solubility of bulk ZnO in pure water is rather low and the published values are quite diverse, ranging from 1.6 to 6.5 mg l^{-1} at 298 K [22]. More recently, a somewhat lower value 0.73 mg l^{-1} at 358 K was reported [23]. The solubility of ZnO increases in both acidic and alkaline solutions and in the presence of a complexing agent (e.g. ammonia, chlorides, sulphates, citrates) [24, 25]. Zn^{2+}, $Zn(OH)^{+}$, $Zn(OH)_2$ and $Zn(OH)_3^-$ are the dominant species in neutral or slightly alkaline aqueous solutions whereas $Zn(OH)_4^{2-}$ becomes important in strongly alkaline solutions in which ZnO solubility is considerably enhanced compared with neutral media. The dissolution of ZnO and Zn^{2+} ion hydrolysis can be described by the following reactions:

$$ZnO(s)+H_2O(l)=Zn^{2+}(aq)+2OH^-(aq) \tag{R1}$$

$$Zn^{2+}(aq)+OH^-(aq)=Zn(OH)^{+}(aq) \tag{R2}$$

$$Zn^{2+}(aq)+2OH^-(aq)=Zn(OH)_2(aq) \tag{R3}$$

$$Zn^{2+}(aq)+3OH^-(aq)=Zn(OH)_3^-(aq) \tag{R4}$$

$$Zn^{2+}(aq)+4OH^-(aq)=Zn(OH)_4^{2-}(aq) \tag{R5}$$

where (aq) denotes the relevant species dissolved in an aqueous solution.

To calculate the equilibrium solubility of ZnO in pure water, the composition of the resulting solution must be evaluated. Here, the non-stoichiometric method, based on minimisation of the total Gibbs energy of the system to the set of points satisfying the material balance conditions, was used to calculate the equilibrium composition of the aqueous solution in equilibrium with solid ZnO. The calculation algorithm and CHEMEQ software have been described elsewhere [26].

The liquid phase was considered as a dilute solution of seven species in H_2O (solvent): H^+, OH^-, Zn^{2+}, $Zn(OH)^{+}$, $Zn(OH)_2$, $Zn(OH)_3^-$ and $Zn(OH)_4^{2-}$. The chemical potentials of the solvent and the solutes were expressed with respect to Raoultian (pure substance) and Henrian (hypothetical ideal solution of the relevant

Table 1 Input thermodynamic data for equilibrium calculations

Substance	$\Delta_f G^\circ$ (298.15), kJ mol^{-1}
H_2O(l)	–237.14
H^+(aq)	0
OH^-(aq)	–157.22
Zn^{2+}(aq)	–147.2
$Zn(OH)^+$(aq)	–342.0
$Zn(OH)_2$(aq)	–528.0
$Zn(OH)_3^-$(aq)	–698.0
$Zn(OH)_4^{2-}$(aq)	–860.0
ZnO(s)	–320.5

solute in water at unit molality) standard states, respectively. The standard Gibbs energies of formation ($\Delta_f G^\circ$) were used as standard chemical potentials (μ°) and these were adopted from the recent assessment by Zhang and Muhammed [27] (Table 1).

To express the non-ideal behaviour of the dilute aqueous solution, the Davies equation for solute activity coefficients γ_i was used [28]

$$\log \gamma_i = -0.509 z_i^2 \left(\frac{\sqrt{I_m}}{1+\sqrt{I_m}} - 0.3 I_m \right) \tag{2}$$

where the Debye–Hückel constant of 0.509 holds for $T = 298.15$ K and the ionic strength on a molal basis I_m is defined as

$$I_m = \frac{1}{2} \sum_{i=1}^{N} m_i z_i^2 \tag{3}$$

Equilibrium calculations were performed at 298.15 K and a standard pressure of 1 bar.

2.2. Dissolution of ZnO nanoparticles: The enhanced dissolution of nanoparticles is due to the interface effect, which results in materials with a large specific interface area having lower thermodynamic stability than the bulk materials. The interface effect can be simply treated by redefining the chemical potential of a solid substance in the form of nanoparticles μ^{np} surrounded by a liquid (fluid in general) phase [29–31]. This holds for general shaped nanoparticles [7, 8]

$$\begin{aligned} \mu^{np} &= \mu^{bulk} + \gamma_{sl} V_m \left(\frac{dA}{dV} \right)_{np} \\ &= \mu^{bulk} + \alpha' \frac{2\gamma_{sl} V_m}{r_{eqv}} \end{aligned} \tag{4}$$

The so called differential shape factor α' [7, 8] is defined as

$$\alpha' = \left(\frac{dA}{dV} \right)_{np} \frac{r_{eqv}}{2} \tag{5}$$

where $r_{eqv} = (3V_{np}/4\pi)^{1/3}$ is the radius of a spherical nanoparticle with the same volume as a non-spherical one. The interfacial energy γ_{sl} is dependent on the composition of the surrounding solution, but in the case of a dilute solution a constant value representing the solid/solvent interface can be used.

The above-described calculation of bulk ZnO solubility in pure water was extended to ZnO nanoparticles of various shapes (spherical as well as hexagonal prisms with different aspect ratios). The chemical potential of ZnO is given as

$$\mu_{ZnO}^{np} = \mu_{ZnO}^{bulk} + \alpha' \frac{2\gamma_{ZnO/water} V_{m,ZnO}}{r_{eqv}} \tag{6}$$

where $\alpha' = 1$ for spherical nanoparticles. In the case of a hexagonal prism (which is a common shape of ZnO(wz) nanoparticles [32, 33]) with a high h and an edge of hexagonal base a with a constant aspect ratio $x = h/a$, the differential shape factor α' is given as

$$\alpha' = \left(\frac{1}{9\pi} \right)^{1/3} \left[\sqrt{3} x^{-2/3} + 2x^{1/3} \right] \tag{7}$$

where $\alpha' = 1.185$ and 1.859 for $x = 2$ and 20, respectively. The value of $V_{m,ZnO} = 14.34 \times 10^{-6}$ m^3 mol^{-1} was used for solid ZnO [34]. Regarding the interfacial energy, the average value $\gamma_{ZnO/water} = 653$ mJ m^{-2} was estimated from contact angle measurements described in the next section.

3. Estimation of the interfacial energy: The interfacial energy $\gamma_{ZnO/water}$ was estimated from the contact angle of the sessile drop of pure water on a ZnO substrate with a polar (000 $\bar{1}$)-O surface. The See System apparatus (Advex, Czech Republic) was used to measure the contact angle θ at $T = 298$ K. The mean value of contact angle $\theta = (90.7 \pm 1.0)°$ was calculated from 35 independent measurements. This is different from the value of 70° obtained for the same surface plane by Xie *et al.* [35]. Higher values of contact angle, namely 109° [36] and 103° [37] were measured on ZnO films with preferential (0001) orientation. The Young's equation

$$\gamma_{ZnO/water} = \gamma_{ZnO} - \gamma_{water} \cos\theta \tag{8}$$

was subsequently used for the calculation of $\gamma_{ZnO/water}$. The generally accepted value for the surface energy of water, $\gamma_{water} = 72.0$ mJ m^{-2}, was used for this calculation [38]. In the case of ZnO, the published values of γ_{ZnO} differ significantly.

Zhang *et al.* [39] determined the surface enthalpy of nanostructured ZnO with different morphologies using calorimetric measurements. Assuming that the entropy term is negligible at 298 K, $\gamma_{ZnO} = 1.31$ J m^{-2} for quasispherical particles with a hydrated surface and $\gamma_{ZnO} = 2.55$ J m^{-2} for an anhydrous one. It follows that water adsorption lowered the surface energy to almost one half of the value for the anhydrous surface. The difference of 1.24 J m^{-2} can be interpreted as the equilibrium spreading pressure. The spreading pressure depends on the crystallographic orientation of the surface and so, for hydrated surfaces, we prefer to apply the ratio of 1.31/2.55 = 0.5 for recalculation of the first-principle calculated γ_{ZnO} values (ZnO(*hkil*)/vacuum interfaces). Nanoparticles with diameters ranging from 14 to 40 nm were used for the experiments to determine the size dependence of surface/interface energy [40].

The value of γ_{ZnO} can be estimated using first-principle calculations. The ability to calculate different γ_{ZnO} values for various (*hkil*) crystallographic planes is the main strength of this approach. Using LDA + U-PAW *ab-initio* calculations, Na and Park [41] calculated the surface energy for low-index (10 $\bar{1}$0), (11 $\bar{2}$0) and (0001) planes (Table 2).

Their value for (10 $\bar{1}$0) planes is in good agreement with *ab-initio* calculated values in the previous studies [42–45]

Table 2 Calculated values of surface energy $\gamma_{ZnO(hkil)}$ and interfacial energy $\gamma_{ZnO(hkil)/water}$

Surface plane	(11$\bar{2}$0)	(10$\bar{1}$0)	(0001)-Zn	(000$\bar{1}$)-O
$\gamma_{ZnO(hkil)}$ as calculated [41], mJ m^{-2}	1060	1120	2250	2040
$\gamma_{ZnO(hkil)}$ (hydrated)[a], mJ m^{-2}	530	560	1125	1020
anisotropy $\gamma_{ZnO(hkil)}/\gamma_{ZnO(11\bar{2}0)}$	1.00	1.06	2.12	1.92
$\gamma_{ZnO(hkil)/water}$[b], mJ m^{-2}	532	564	1127	1021

[a]Obtained as one half of calculated values $\gamma_{ZnO(hkil)}$ for ZnO/vacuum interface.

[b]Calculated using $\gamma_{ZnO(000\bar{1})/water} = 1021$ J m^{-2} and anisotropy coefficients.

doi: 10.1049/mnl.2018.5158

(differences 3–15%) but the surface energy for the (11 $\bar{2}$0) plane is slightly underestimated.

The calculated values refer to the ZnO/vacuum interface. We estimated the surface energies of the hydrated surfaces on the basis of the above-mentioned experimental findings [39]. Assuming that $\gamma_{ZnO(hkil)}$(hydrated) = $\gamma_{ZnO(hkil)}/2$, for (000 1)-O we obtained $\gamma_{ZnO(000\bar{1})}$(hydrated) = 1020 mJ m^{-2}. Furthermore, with respect to the lowest energy plane (11$\bar{2}$0), anisotropy coefficients defined as $\gamma_{ZnO(hkil)}/\gamma_{ZnO(11\bar{2}0)}$ were calculated. Using Young's equation (8) with a contact angle of $\theta = 90.7°$ and $\gamma_{water} = 72.0$ mJ m^{-2}, $\gamma_{ZnO(000\bar{1})/water} = 1021$ mJ m^{-2} was obtained. The interfacial energies for other surface planes were calculated using this value and assuming the same anisotropy coefficients as for the surface energies $\gamma_{ZnO(hkil)}$ (see Table 2).

The real shape of ZnO(wz) nanoparticles is a hexagonal prism with bases formed by polar (0001)-Zn and (000$\bar{1}$)-O planes and faces formed by non-polar (10$\bar{1}$0) and/or (11$\bar{2}$0) planes [32, 33]. From a strictly geometrical viewpoint, the ratio of the height h to the length of basal edges a which minimises the surface-to-volume ratio of such a prism is $h = \sqrt{3}a$ with the bases representing 33.3% of the total surface area. However, this only holds for a completely isotropic surface; appreciable surface energy anisotropy moves this ratio to higher values. Based on the Wulff calculation (minimisation of the total surface Helmholtz energy), we obtained $h/a = 3.46$, which resulted in 20% part of the total surface area for bases and 80% for faces. These parts were used as weights for calculating the average interfacial energy, $\gamma_{ZnO/water} = 653$ mJ m^{-2}.

4. Results and discussion: The calculated solubility of bulk ZnO at $T = 298.15$ K was $c_{ZnO} = 1.15$ mg l^{-1} ($c_{Zn} = 0.924$ mg l^{-1}). The pH of the resulting solution was 8.9 and the corresponding ionic strength $I_m = 8.2 \times 10^{-6}$. The most abundant species was $Zn(OH)^+$ which retained 52.6% of the entire Zn content in the solution. The effect of size and shape on ZnO solubility is presented in Fig. 1. When the size of the spherical nanoparticles was reduced to 2 nm in radius, the solubility was enhanced by a factor of 23.7 compared with the bulk ZnO. At the same time, pH of the resulting solution increased to 9.7 and $Zn(OH)_2$(aq) became the predominant species in the aqueous solution. These results were compared with the values predicted using the Ostwald–Freundlich equation (1) in the form

$$\frac{c_{ZnO,np}}{c_{ZnO,bulk}} = \exp\left(\frac{2\gamma_{ZnO/water}V_{m,ZnO}}{RTr}\right) = \exp\left(\frac{7.293}{r/nm}\right) \quad (9)$$

Slight differences exist for nanoparticles with radii lower than ~10 nm. These differences can be explained in terms of the complex chemistry in aqueous ZnO solutions while the Ostwald–Freundlich equation assumes a simple dissolution process.

Additional calculations were carried out for the hexagonal prism nanoparticles with different a and h parameters but at constant values of $x = h/a = 2$ and 20. As these nanoparticles exhibited higher surface-to-volume ratios than the spherical ones, a further increase in ZnO solubility could be anticipated (see Fig. 1).

It is also possible to estimate the influence of changing the ionic strength of an aqueous solution on ZnO solubility. Assuming that the addition of inert ionic species increases the ionic strength (without any Zn^{2+} complexation, e.g. some pH buffer), the activity coefficients of the dissolved species calculated by (2) decrease and the concentrations of those species in solution thus increase. However, this effect only became significant at a relatively high ionic strength ($I_m > 0.1$).

The effect of ionic strength becomes important when we try to estimate the solubility of ZnO as a function of pH, which can be varied by the addition of an acid or a base with no or negligible complexation ability towards Zn^{2+}. Simulating pH lowering by the addition of 0.2 mol HCl (neglecting all chloridocomplexes of Zn^{2+}), we obtained a solubility of 8.2 g ZnO/L at pH = 6.4 for bulk ZnO. The reduction in the size of spherical nanoparticles to 2 nm in radius led to a shift to 9.0 g ZnO/L and pH = 7.2. The corresponding ionic strength, $I_m = 0.3$, was still in the range in which Davies's equation can be applied. In contrast, increasing pH by NaOH addition (0.2 mol) resulted in the shift of ZnO solubility from 0.06 g ZnO/L (pH = 13.2) to 1.9 g ZnO/L (pH = 13.1) for bulk and 2 nm sized ZnO, respectively.

It should be noted that there are some areas of concern regarding our calculations. In particular, there are some uncertainties in terms of the input thermodynamic data including the value of ZnO/aqueous solution interface energy. Moreover, the particle shapes considered were idealised, their equilibrium sizes differed from real ones. Neither particle aggregation nor transport nor the kinetic limitations of the dissolution process were considered here, which means that the presented solubilities correspond to a long-term exposure of free particles to aqueous media.

Our results, obtained on the basis of a simple thermodynamic model, can be compared with literature data for the effect of size on nano-ZnO solubility (Fig. 2). Direct comparison with experimental data can be rather confusing as the solubility measurements have been performed at various values of pH in solvents with

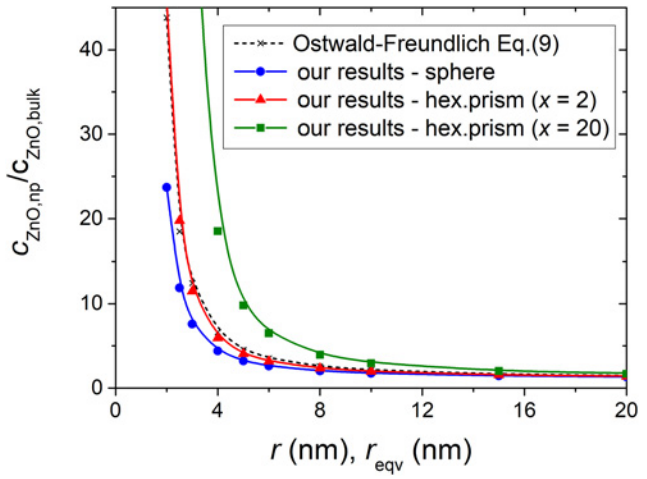

Fig. 1 *Equilibrium solubility of ZnO nanoparticles of radius r or equivalent radius r_{eqv} in pure water*

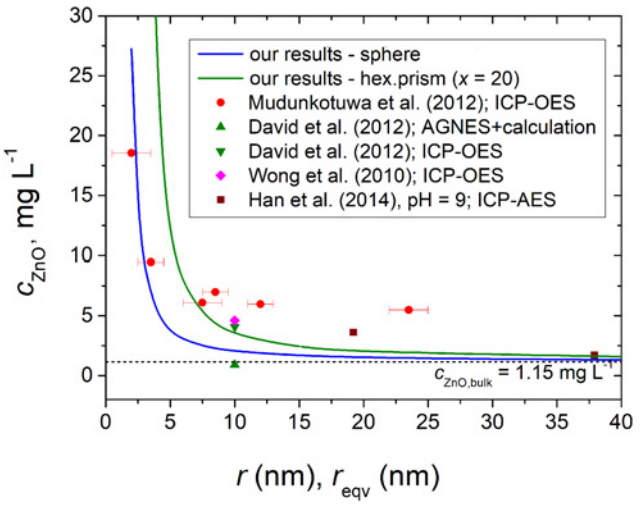

Fig. 2 *Comparison of predicted size effect on ZnO solubility with experimental data of Mudunkotuwa et al. [11], David et al. [12], Wong et al. [4], Han et al. [15]*

Zn^{2+} complexation ability, making ZnO solubility higher than in pure water. Using the relative expression $c_{ZnO,np}/c_{ZnO,bulk}$ for the comparison would be indeed better than using absolute values of $c_{ZnO,np}$, but in most papers bulk solubility in the relevant solvents was not determined. It is also worth mentioning that in some papers it is not explicitly stated whether the total zinc concentrations in relevant solutions correspond to equilibrium, steady-state or time-dependent values. Furthermore, particle dimensions are reported before solubility experiments during which the original size can be decreased (due to dissolution) or increased (due to aggregation). Experimental results are also strongly dependent on the methods used for separating the undissolved particles from the solution and for determining the zinc content in the solution.

Mudunkotuwa *et al.* [11] measured ZnO solubility in water at $T = 298$ K and pH = 7.5. The pH value was set using HEPES organic buffer without any complexation ability. The total Zn content in aqueous solution, obtained by ultrafiltration of the suspension, was determined by inductively coupled plasma optical emission spectroscopy (ICP-OES) method. Their results (Fig. 2) are in good agreement with our thermodynamic prediction for nanoparticles with radii of 2 and 3.5 nm, but the solubilities they obtained for larger nanoparticles were approximately four times higher than our values. Assuming the solubility for the largest particles ($r = 65$ nm) $c_{ZnO} = 4.2$ mg l^{-1} did not differ significantly from the bulk value, we can estimate $\gamma_{ZnO/water}$ using (9). For nanoparticles with radii of 2 or 3.5 nm $\gamma_{ZnO/water} = 255$ mJ m^{-2} and 243 mJ m^{-2} was obtained, these values seem to be rather low, only reaching approximately 40% of our values.

David *et al.* [12] measured ZnO nanoparticle solubility in KCl and KNO_3 aqueous solutions with a total ionic strength of 0.1 at 298.15 K. The free Zn^{2+}(aq) concentrations were determined using the AGNES electroanalytical method and the total Zn content in the solution was calculated from the Zn^{2+}(aq) concentration, solution pH and relevant stability constants for Zn hydroxido complexes. For nanoparticles of $r = 10$ nm at pH = 8.3, a solubility of $c_{ZnO} = 0.91$ mg l^{-1} was obtained, which is lower than our value for bulk ZnO. In contrast, they obtained a nearly fourfold higher value, $c_{ZnO} = 4.07$ mg l^{-1}, using ultrafiltration and ICP-OES, which is comparable to our calculated value, $c_{ZnO} = 2.02$ mg l^{-1}.

Wong *et al.* [4] measured ZnO solubility in artificial seawater (pH = 8, $I_m = 0.5$) at 298 ± 2 K. While the bulk ZnO solubility determined by ultrafiltration and ICP-OES was 2.0 mg l^{-1}, enhanced solubility ($c_{ZnO} = 4.6$ mg l^{-1}) was observed for the ZnO nanoparticles ($r = 10$ nm). This was probably due to the relatively high ionic strength.

Conversely, some papers have reported similar solubilities for bulk and nano-ZnO. For example, Franklin *et al.* [16] measured the solubility of bulk and nano-ZnO ($r = 15$ nm) in 0.01 M Ca $(NO_3)_2$ solution in Milli-Q water buffered to pH = 7.5. The equilibrium solubility 19.9 mg l^{-1} of both forms of ZnO was determined using an equilibrium dialysis method.

5. Conclusion: In this work, we have used a combined experimental and theoretical approach to assess the average interfacial energy of spherical ZnO nanoparticles in water. Our assessment is based on measuring the contact angle of water on a ZnO substrate, on literature data for surface energies obtained by calorimetry measurements and on ab-initio calculations, as well as on using the Wulff construction for optimal hexagonal shape by minimising the free energy with respect to the surface areas of the respective crystallographic planes.

To calculate the equilibria in systems with ZnO nanoparticles, the chemical potential of ZnO was modified by including a surface term. The differential shape factor was used so that the chemical potential of ZnO can be expressed for various particle sizes and shapes. Equilibria comprising ZnO nanoparticles and aqueous solutions were calculated using the Gibbs energy minimisation algorithm. The activities of the zinc(II) species dissolved in aqueous solutions were calculated by the extended Debye–Hückel model (Davies equation).

An appreciable enhancement of the equilibrium concentration of the dissolved species was found, being 23.7 times higher value for 2 nm spherical particles than for bulk ZnO material. For hexagonal prismatic particles with a high surface-to-volume ratio, this effect is even more significant. At present, our thermodynamic model does not consider dissolution as a dynamic process during which particle size decreases; rather, the equilibrium state of the system under investigation is predicted. Despite this limitation, the present calculations clearly point to the notable nanosizing effect of ZnO solubility in aqueous media.

It is very difficult, if not impossible, to precisely determine the size of ZnO nanoparticles that can be considered 'safe' in health and environmental terms [46]. The main reasons for this are: (i) only nominal concentrations of ZnO nanoparticles in suspensions are given in most publications (instead of the dissolved Zn content), (ii) size-dependent toxic effects of ZnO nanoparticles are still not clear, though it has been confirmed that the direct activity of both undissolved particles and Zn^{2+} ions in aqueous media contribute and (iii) the toxic effects of ZnO nanoparticles towards various kinds of living organisms are quite different.

6. Acknowledgment: This work was supported by the Czech Science Foundation, grant no. 17-13161S.

7 References

[1] Moezzi A., McDonagh A.M., Cortie M.B.: 'Zinc oxide particles: synthesis, properties and applications', *Chem. Eng. J.*, 2012, **185**, (Supplement C), pp. 1–22
[2] Prasad A.S.: 'Zinc in human health: effect of zinc on immune cells', *Mol. Med.*, 2008, **14**, (5–6), pp. 353–357
[3] Broadley M.R., White P.J., Hammond J.P., *et al.*: 'Zinc in plants', *New Phytol.*, 2007, **173**, (4), pp. 677–702
[4] Wong S.W., Leung P.T., Djurišić A., *et al.*: 'Toxicities of nano zinc oxide to five marine organisms: influences of aggregate size and ion solubility', *Anal. Bioanal. Chem.*, 2010, **396**, (2), pp. 609–618
[5] Li J., Schiavo S., Rametta G., *et al.*: 'Comparative toxicity of nano ZnO and bulk ZnO towards marine algae Tetraselmis Suecica and Phaeodactylum Tricornutum', *Environ. Sci. Pollut. Res.*, 2017, **24**, (7), pp. 6543–6553
[6] Bacchetta R., Maran B., Marelli M., *et al.*: 'Role of soluble zinc in ZnO nanoparticle cytotoxicity in Daphnia Magna: a morphological approach', *Environ. Res.*, 2016, **148**, pp. 376–385
[7] Leitner J., Sedmidubský D.: 'Thermodynamic equilibria in systems with nanoparticles', in 'Thermal physics and thermal analysis' (Springer, Switzerland, 2017)
[8] Leitner J., Sedmidubský D.: 'Enhanced solubility of nanostructured paracetamol', *Biomed. Phys. Eng. Express*, 2016, **2**, (5), p. 055007
[9] Meulenkamp E.A.: 'Size dependence of the dissolution of ZnO nanoparticles', *J. Phys. Chem. B*, 1998, **102**, (40), pp. 7764–7769
[10] Bian S.-W., Mudunkotuwa I.A., Rupasinghe T., *et al.*: 'Aggregation and dissolution of 4 Nm ZnO nanoparticles in aqueous environments: influence of Ph, ionic strength, size, and adsorption of humic acid', *Langmuir*, 2011, **27**, (10), pp. 6059–6068
[11] Mudunkotuwa I.A., Rupasinghe T., Wu C.-M., *et al.*: 'Dissolution of ZnO nanoparticles at circumneutral Ph: a study of size effects in the presence and absence of citric acid', *Langmuir*, 2011, **28**, (1), pp. 396–403
[12] David C.A., Galceran J., Rey-Castro C., *et al.*: 'Dissolution kinetics and solubility of ZnO nanoparticles followed by Agnes', *J. Phys. Chem. C*, 2012, **116**, (21), pp. 11758–11767
[13] Henkler F., Tralau T., Tentschert J., *et al.*: 'Risk assessment of nanomaterials in cosmetics: a European union perspective', *Arch. Toxicol.*, 2012, **86**, (11), pp. 1641–1646
[14] Reed R.B., Ladner D.A., Higgins C.P., *et al.*: 'Solubility of nano-zinc oxide in environmentally and biologically important matrices', *Environ. Toxicol. Chem.*, 2012, **31**, (1), pp. 93–99
[15] Han Y., Kim D., Hwang G., *et al.*: 'Aggregation and dissolution of ZnO nanoparticles synthesized by different methods: influence of ionic strength and Humic acid', *Colloids Surf. A, Physicochem. Eng. Aspects*, 2014, **451**, pp. 7–15
[16] Franklin N.M., Rogers N.J., Apte S.C., *et al.*: 'Comparative toxicity of nanoparticulate ZnO, bulk ZnO, and Zncl2 to a freshwater

doi: 10.1049/mnl.2018.5158

microalga (Pseudokirchneriella Subcapitata): the importance of particle solubility', *Environ. Sci. Technol.*, 2007, **41**, (24), pp. 8484–8490
[17] Miao A.J., Zhang X.Y., Luo Z., *ET AL.*: 'Zinc oxide–engineered nanoparticles: dissolution and toxicity to marine phytoplankton', *Environ. Toxicol. Chem.*, 2010, **29**, (12), pp. 2814–2822
[18] Odzak N., Kistler D., Behra R., *ET AL.*: 'Dissolution of metal and metal oxide nanoparticles in aqueous media', *Environ. Pollut.*, 2014, **191**, pp. 132–138
[19] Wang D., Lin Z., Wang T., *ET AL.*: 'Where does the toxicity of metal oxide nanoparticles come from: the nanoparticles, the ions, or a combination of both?', *J. Hazard. Mater.*, 2016, **308**, pp. 328–334
[20] Majedi S.M., Kelly B.C., Lee H.K.: 'Combined effects of water temperature and chemistry on the environmental fate and behavior of nanosized zinc oxide', *Sci. Total Environ.*, 2014, **496**, pp. 585–593
[21] Peng Y.-H., Tsai Y.-C., Hsiung C.-E., *ET AL.*: 'Influence of water chemistry on the environmental behaviors of commercial ZnO nanoparticles in various water and wastewater samples', *J. Hazard. Mater.*, 2017, **322**, pp. 348–356
[22] Clever H.L., Derrick M.E., Johnson S.A.: 'The solubility of some sparingly soluble salts of zinc and cadmium in water and in aqueous electrolyte solutions', *J. Phys. Chem. Ref. Data*, 1992, **21**, (5), pp. 941–1004
[23] Palazhchenko O.: 'Pourbaix diagrams at elevated temperatures: a study of Zn and Sn', 2012
[24] Chen A.-L., Xu D., Chen X.-Y., *ET AL.*: 'Measurements of zinc oxide solubility in sodium hydroxide solution from 25 to 100°C', *Trans. Nonferr. Met. Soc. China*, 2012, **22**, (6), pp. 1513–1516
[25] Ding Z.-Y., Chen Q.-Y., Yin Z.-L., *ET AL.*: 'Predominance diagrams for Zn (II)–NH_3–Cl−−H_2O system', *Trans. Nonferr. Met. Soc. China*, 2013, **23**, (3), pp. 832–840
[26] Voňka P., Leitner J.: 'Calculation of chemical equilibria in heterogeneous multicomponent systems', *Calphad*, 1995, **19**, (1), pp. 25–36
[27] Zhang Y., Muhammed M.: 'Critical evaluation of thermodynamics of complex formation of metal ions in aqueous solutions: VI. Hydrolysis and hydroxo-complexes of Zn2+ at 298.15 K', *Hydrometallurgy*, 2001, **60**, (3), pp. 215–236
[28] Barry T.I.: 'Chemical thermodynamics in industry: models and computation' (Blackwell Science Incorporated, London, 1985)
[29] Yongqiang X., Baojiao G., Jianfeng G.: 'The theory of thermodynamics for chemical reactions in dispersed heterogeneous systems', *J. Colloid Interface Sci.*, 1997, **191**, (1), pp. 81–85
[30] Wu W., Nancollas G.H.: 'A new understanding of the relationship between solubility and particle size', *J. Solution Chem.*, 1998, **27**, (6), pp. 521–531
[31] Schäfer R.: 'The chemical potential of metal atoms in small particles', 2003
[32] Fan H.J., Barnard A.S., Zacharias M.: 'ZnO nanowires and nanobelts: shape selection and thermodynamic modeling', *Appl. Phys. Lett.*, 2007, **90**, (14), p. 143116
[33] Große Holthaus S., Köppen S., Frauenheim T., *ET AL.*: 'Atomistic simulations of the ZnO (1210)/water interface: a comparison between first-principles, tight-binding, and empirical methods', *J. Chem. Theory Computat.*, 2012, **8**, (11), pp. 4517–4526
[34] Desgreniers S.: 'High-density phases of ZnO: structural and compressive parameters', *Phys. Rev. B*, 1998, **58**, (21), p. 14102
[35] Xie S., Zhao Y., Jiang Y.: 'Laser-induced hydrophobicity on single crystal zinc oxide surface', *Appl. Surf. Sci.*, 2012, **263**, pp. 405–409
[36] Sun R.-D., Nakajima A., Fujishima A., *ET AL.*: 'Photoinduced surface wettability conversion of ZnO and TiO_2 thin films', *J. Phys. Chem. B*, 2001, **105**, (10), pp. 1984–1990
[37] Huang L., Lau S., Yang H., *ET AL.*: 'Stable superhydrophobic surface via carbon nanotubes coated with a ZnO thin film', *J. Phys. Chem. B*, 2005, **109**, (16), pp. 7746–7748
[38] Vargaftik N., Volkov B., Voljak L.: 'International tables of the surface tension of water', *J. Phys. Chem. Ref. Data*, 1983, **12**, (3), pp. 817–820
[39] Zhang P., Xu F., Navrotsky A., *ET AL.*: 'Surface enthalpies of nanophase ZnO with different morphologies', *Chem. Mater.*, 2007, **19**, (23), pp. 5687–5693
[40] Jiang Q., Lu H.: 'Size dependent interface energy and its applications', *Surf. Sci. Rep.*, 2008, **63**, (10), pp. 427–464
[41] Na S.-H., Park C.-H.: 'First-principles study of the surface energy and the atom cohesion of Wurtzite ZnO and ZnS-implications for nanostructure formation', *J. Korean Phys. Soc.*, 2010, **56**, (12), pp. 498–502
[42] Marana N., Longo V., Longo E., *ET AL.*: 'Electronic and structural properties of the (1010) and (1120) ZnO surfaces', *J. Phys. Chem. A*, 2008, **112**, (38), pp. 8958–8963
[43] Cooke D.J., Marmier A., Parker S.C.: 'Surface structure of (1010) and (1120) surfaces of ZnO with density functional theory and atomistic simulation', *J. Phys. Chem. B*, 2006, **110**, (15), pp. 7985–7991
[44] Meyer B., Marx D.: 'Density-functional study of the structure and stability of ZnO surfaces', *Phys. Rev. B*, 2003, **67**, (3), p. 035403
[45] Wander A., Harrison N.: 'An *ab initio* study of ZnO (1010)', *Surf. Sci.*, 2000, **457**, (1), pp. L342–L346
[46] Hou J., Wu Y., Li X., *ET AL.*: 'Toxic effects of different types of zinc oxide nanoparticles on algae, plants, invertebrates, vertebrates and microorganisms', *Chemosphere*, 2018, **193**, pp. 852–860